NRL Report 3062

Brightness and Two-Color Pyrometry Applied to the Electron Beam Furnace

H. Doering and P. Shahinian

High Temperature Alloys Branch
Metallurgy Division

June 10, 1964

U.S. NAVAL RESEARCH LABORATORY
Washington, D.C.

CONTENTS

BLANK PAGE

Brightness and Two-Color Pyrometry Applied to the Electron Beam Furnace

H. Doering and P. Shahinian

High Temperature Alloys Branch
Metallurgy Division

A procedure for temperature measurement and control in an electron beam furnace was established by using the optical and two-color pyrometers. The emissivity of the specimen and attenuation by the furnace sight-port glass and metallic vapor coatings introduced errors in the readings made by both instruments. These errors in two-color readings were considerably less than those in readings made with the optical pyrometer. To permit the determination of the true temperature of a test specimen, an empirical correlation was made between the temperature of a blackbody hole and the brightness of a surface simulating that of a test specimen. The accuracy of this correlation is discussed with respect to the quality of the blackbody holes, the errors in sight-port glass corrections, instrument calibration, and the accumulated statistical uncertainties of pyrometer readings.

INTRODUCTION

A facility to evaluate the mechanical properties of refractory metals up to a temperature of 6000°F was recently put into operation at this Laboratory. The equipment, consisting of an electron beam furnace attached to an Instron tester, permits tensile, compression, relaxation, and low-cycle fatigue testing. Heating of the test specimen is accomplished by bombardment of the specimen surfaces by electron beams generated in two self-accelerating electron guns. The desired temperature is obtained by adjusting the emission current in each gun, and the beams are swept over the specimen to obtain an even temperature distribution.

It was the purpose of this study to evaluate pyrometric instruments for the determination of temperature in the electron beam furnace, as well as to establish a reliable procedure for making the temperature measurements. Also, the statistical uncertainty of such measurements was evaluated.

INSTRUMENTS AVAILABLE FOR HIGH-TEMPERATURE MEASUREMENT

The more common instruments used for high-temperature measurement were considered for possible use with the electron beam furnace. They include thermocouples, total radiation pyrometers, optical pyrometers, and two-color pyrometers.

NRL Problem M01-09, Project RR-007-01-46-5407, NRPA Order 1158(1). This report completes one phase of the problem; work on other phases of the problem is continuing. Manuscript submitted December 30, 1963.

Thermocouples, although convenient for both measurement and control, are limited, at best, to about 4500°F. Furthermore, they cannot be exposed to the electron beam since the introduction of electrical currents would cause errors in the temperature measurements.

Total radiation pyrometers may be used for measurement and control at higher temperatures, but they are subject to very serious error when (a) the emissivity of the specimen is not accurately known, (b) there are contaminants present in the atmosphere, and (c) the furnace sight-port glass becomes coated with metallic vapors from the heated specimen.

The disappearing-filament optical pyrometer, because of its higher accuracy and stability, is more frequently used for high-temperature measurements (1). Readings of this instrument, which is calibrated for blackbody conditions, usually must be corrected for the target's emissivity and for attenuators such as sight glasses and coatings.

The two-color pyrometer, which can provide continuous measurement and control, overcomes some of the errors which are common to optical pyrometer readings (2,3). The instrument directly measures the ratio of intensities emitted within two different wavelength bands—the intensity within a band in the blue region of the spectrum to the intensity within a band in the red region of the spectrum. When a sighting is made on a blackbody, this ratio increases with increasing temperature according to Planck's radiation law. The instrument is so constructed that this ratio is read directly as temperature. Because this pyrometer

utilizes the ratio of energy emitted within two wavelength bands rather than the magnitude of energy within only one band, it should be relatively insensitive to differences in emissivity (which is a function of wavelength), contaminants in the atmosphere, and attenuation by sight glasses and coatings. It is indeed insensitive to these factors when the spectral emissivities are equal within the two wavelength bands (graybody emission) and when the spectral attenuations within each wavelength band are equal in both the glass and the coating. In reality, these conditions rarely exist and some error is introduced. For example, if more blue than red is emitted from a surface in comparison to that emitted by a blackbody, then the temperature reading will be higher than true temperature. Similarly, if the sight glass transmits less blue than red radiation, the temperature will read lower than it would if no sight glass were present. The instrument possesses very high sensitivity, and this attribute makes it particularly suitable for the continuous monitoring and control of temperature.

On the basis of their inherent characteristics, the optical and two-color pyrometers were selected for evaluation to determine their suitability for temperature measurement in the electron beam furnace.

EXPERIMENTAL TEMPERATURE DETERMINATION

General Approach

The factors that influence temperature measurement in the electron beam furnace include emissivity, furnace reflections, and attenuation by the sight glass and coatings. These factors are examined in detail as they affect readings taken with the optical pyrometer, together with considerations of instrument calibration and reading uncertainties.

Published values of emissivity for tungsten cannot be used with confidence in the electron beam furnace since these values apply only to polished surfaces sighted perpendicularly. The test specimens used in this furnace may be either rod or sheet and are machined to finishes having a certain degree of roughness. Also, sheet specimens cannot be viewed perpendicularly (Fig. 1), as can the rod specimens. For these reasons, together with the consideration of furnace

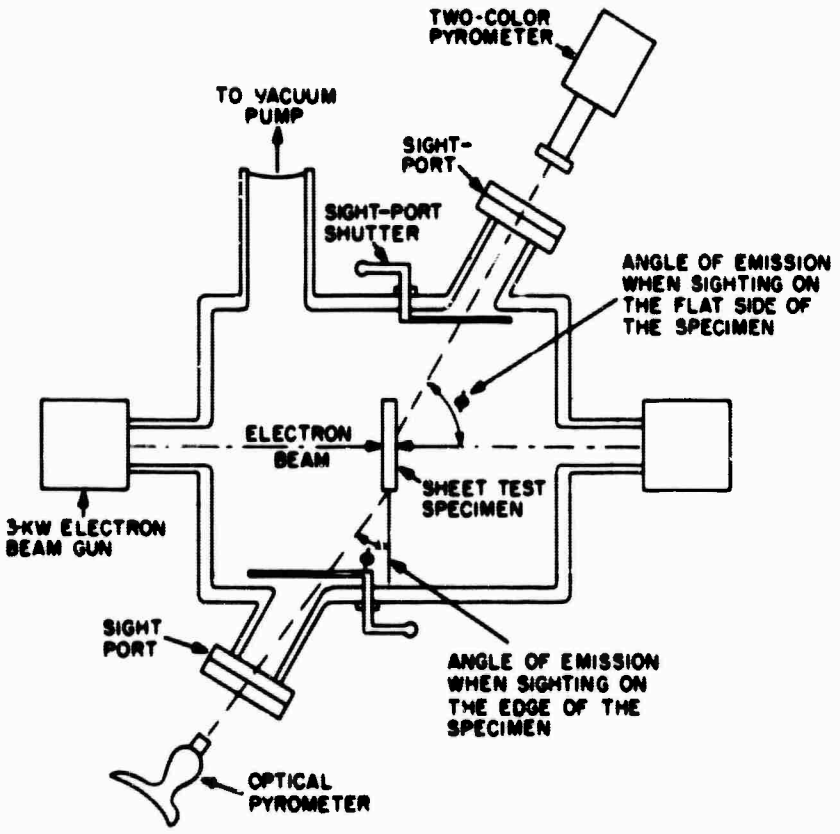

Fig. 1 - Schematic plan view of electron beam furnace

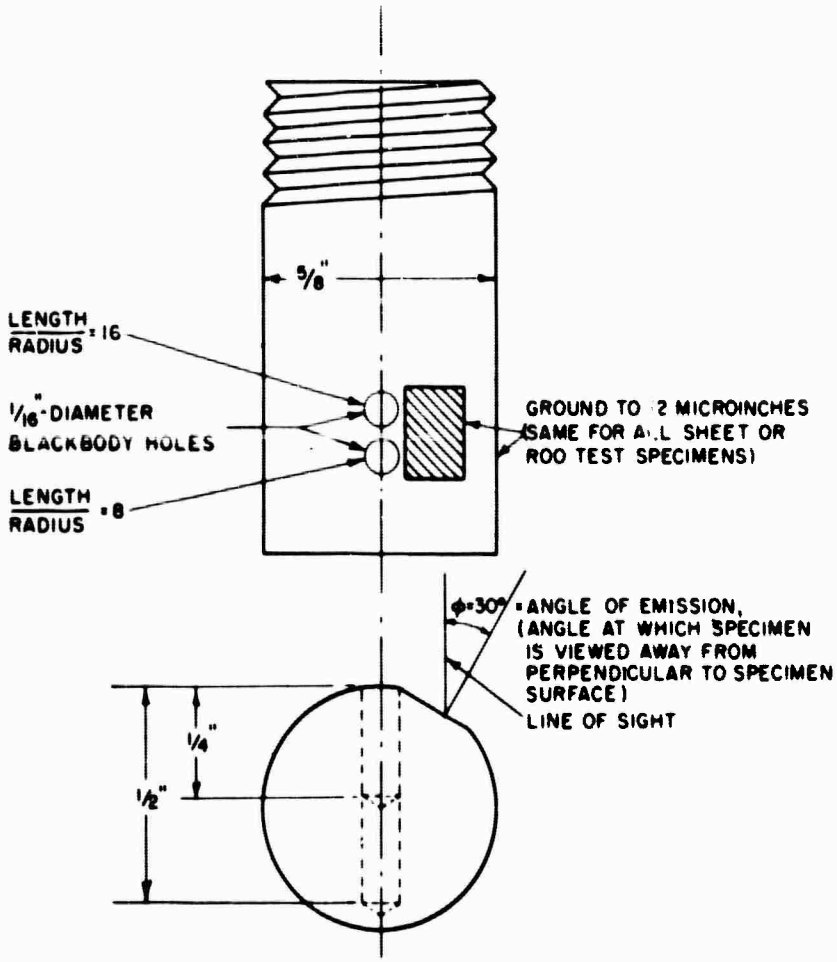

Fig. 2 - Dummy tungsten specimen with blackbody holes used for the determination of specimen emissivity

reflections, an empirical approach to the establishment of true temperature is adopted. This is accomplished by making the comparision between a blackbody and a surface at the same temperature, the surface being similar to that of the sheet test specimen where all the possible variables are encountered.

The effects of emissivity and of attenuation by sight glass and coatings on the two-color pyrometer readings are determined and compared to the effects on the optical pyrometer readings. From this comparison, and from considerations of the basic characteristics of each instrument, a procedure is established for both the determination of the true temperature and the monitoring and control during a test.

Optical Pyrometry

Correction for Emissivity—The emissivity ϵ, defined as the ratio of the total radiant energy emitted from a surface to the total energy emitted by a blackbody at the same temperature, depends on temperature, material, surface finish, and the angle of emission. To establish the emissivity of a test specimen, an experiment was devised which would account for all the variables upon which emissivity is dependent, including reflections from within the furnace. A dummy specimen of tungsten was constructed as shown in Fig. 2 in order to establish the relationship between the blackbody (or true) temperature and the surface brightness temperature. The two holes of length-to-radius (L/R) ratios of 16 and 8 are designed to provide blackbody conditions.

Theoretically, the hole with a L/R ratio of 16 should radiate 0.964 to 0.997 of the energy of a blackbody and the hole with a L/R ratio of 8 should radiate 0.866 to 0.990 the energy (4). No difference in brightness was observed between the two holes, so at best they radiate 0.990 of the

TABLE I
Theoretical Temperature Difference ($T - T_{obs}$) Owing to Departure of Dummy Tungsten Specimen Holes from Blackbody Conditions

Blackbody Temperature T (°K)	$T - T_{obs}$ According to DeVos (4) (°K)		$T - T_{obs}$ According to Casselton *et al.* (5) (°K)	
	For L/R=16	For L/R=8	For L/R=16	For L/R=8
1000	1	2	2	5
2000	2	6	7	26
3000	4	14	16	57
4000	7	27	29	103

energy of a blackbody and at worst they radiate 0.964 of that energy. The resulting theoretical temperature differences, due to departure from blackbody conditions, are given by Wien's law at a wavelength of 0.65 micron as

$$\frac{1}{T} - \frac{1}{T_{obs}} = \frac{\log f}{9606} \qquad (1)$$

and are tabulated for four values of true temperature in Table 1. In Eq. (1) T is the true (blackbody) temperature, T_{obs} is the observed brightness temperature of the hole, and f is the theoretical fraction of blackbody radiation from the hole. Wien's law is simpler than Planck's law and is a close approximation to it at the wavelengths and temperatures discussed here.

Casselton *et al.* (5) have provided another means of calculating the theoretical departure from blackbody brightness. The relation they developed is based on the geometry of the holes and the emissivity of the material in which the holes are drilled. This departure is given by

$$T - T_{obs} = \frac{T^2}{9606}\log\left[1 + \frac{(1-\epsilon_\lambda)}{\epsilon_\lambda}\cdot\frac{1}{2(L/R)}\right]. \qquad (2)$$

Assuming that the spectral emissivity ϵ_λ at $\lambda = 0.65$ micron is 0.45 for tungsten, the departures of both 1/16-in.-diam holes in the dummy specimen are also listed in Table 1.

In the present work, however, the holes will be assumed to be blackbodies since the errors would be small and since both holes appeared equally bright. Furthermore, a thermocouple placed inside another dummy specimen 1/16 in. away from the blackbody hole gave agreement to within a few degrees of the optical pyrometer readings over the interval 1300-1500°C. Thus, the assumption that the holes are blackbodies is further supported.

In order to simulate the surface of a test specimen, a flat surface on the cylindrical dummy specimen was provided so as to have the same angle of emission (as defined in Fig. 1) and the same surface finish (12 microinches) as that of the narrow edge of the test specimens to be used in the furnace. The increase of the spectral emissivity with increasing angle of emission up to a maximum at 75 degrees is shown at two wavelengths for tungsten (6) in Fig. 3. Readings of a blackbody temperature and a corresponding surface brightness temperature T_B on the dummy specimen will permit a calculation of the spectral emissivity ϵ_λ at a given wavelength. For a number of measured temperatures, the values of ϵ_λ were computed from the relationship

$$T_B - T = \frac{2.303\,T_B\,T\,\lambda\log\epsilon_\lambda}{C_2} \qquad (3)$$

where C_2 = 14,833 microns-°K and λ = 0.65 micron. These values, shown in Table 2, differ from reported values for polished tungsten viewed perpendicularly to the surface. For example, at a temperature in the vicinity of 2000°C, Table 2 shows a value $\epsilon_{\lambda=0.65} = 0.47$, in contrast to reported values of 0.44 (7) and 0.37 (8). But the values shown in Table 2 were found reproducible; hence they may be assumed correct for the furnace reflections, specimen finish, and angle of emission present here.

TABLE 2
Selected Values of Factors Influencing the Measurement of Specimen Temperature by the Type of Pyrometer Indicated

Blackbody Temperature* (°C)	Sheet Specimen Surface Temperature* (°C)		Glass Attenuation Correction		Spectral Emissivity $\epsilon_{\lambda=0.65}$	Spectral Transmittance per 1.4-in. Pyrex $\tau_{\lambda=0.65}$
	Optical Pyrometer ($\phi = 30°$†)	Two-Color Pyrometer‡ ($\phi = 60°$)	Optical Pyrometer (°C)	Two-Color Pyrometer (°C)		
1267	1210	1242	10	2	0.57	0.904
1515	1420	1480	13	3	0.50	0.907
1776	1643	1665	17	4	0.47	0.907
2035	1870	1980	20	5	0.47	0.914
2295	2090	2205	23	6	0.47	0.919
2557	2300	2480	27	7	0.46	0.921
2799	2490	2750	30	8	0.45	0.926
3100	2720	3080	33	9	0.44	0.929

*Corrected for sight port glass attenuation
†ϕ = angle of emission as defined in Fig. 1
‡Two-color readings are corrected to true temperature as if target had been polished tungsten sighted perpendicularly to surface (Ref. (9))

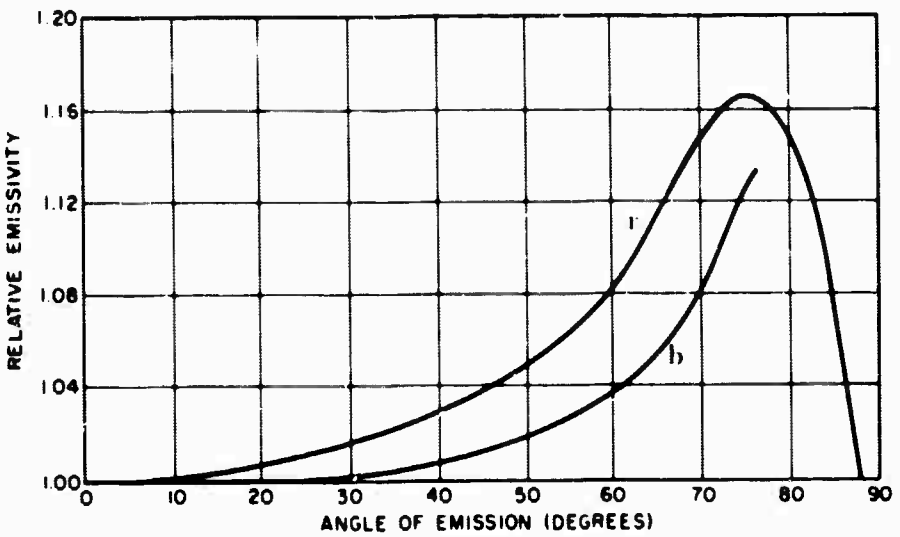

Fig. 3 - Variation in relative spectral emissivity with angle of emission for tungsten. Measurements were made at (a) $\lambda = 0.66$ micron (red), and (b) $\lambda = 0.47$ micron (blue) (data from Ref. (6)). Note that $\lambda = 0.66$ micron is neither the wavelength used by the optical pyrometer (0.65 micron) nor the red used by the two-color pyrometer (0.64 micron).

Sight Glass Correction — The true temperature is the reading of the blackbody holes in the dummy specimen after correcting for attenuation by the sight-port glass. The attenuation by the sight glass is due, in large part, to reflections from the surfaces of the glass. To a lesser extent, the attenuation is dependent on the absorption of light by the glass itself and to the scattering of light by imperfections.

Among several methods used to correct for the attenuation by the sight glass, the following procedure was found convenient and reliable.

A temperature T_1 is measured through the single glass (1/4-in. Pyrex). Next, an identical glass is interposed in the line of sight and the resulting drop in temperature $(T_1 - T_2)$ becomes the glass correction for T_2 only, and not for T_1 as is frequently assumed. Using $(T_1 - T_2)$ as the correction for T_1 would introduce an error of 1.1°K at 3000°K. This error is due in part to multiple reflections and in part to the fact that the correction $(T_1 - T_2)$ decreases with decreasing brightness, and since the second piece of glass sees a lower brightness than the first, the correction $(T_1 - T_2)$ is low when applied to T_1. Hence, plotting T_2 versus $(T_1 - T_2)$ for different specimen temperatures provides a more accurate empirical correction for a sight-port glass. When a brightness temperature is measured through the sight-port glass, the corresponding plotted correction for that temperature is added to the measured brightness to find the brightness as if no glass were present.

In the above empirical procedure, multiple reflections between the two glasses also introduce an error. The four surfaces of the two glasses make it possible for more light to be transmitted through the second glass than through the first so that the empirical correction for the second is inevitably measured lower than for the first. But if one assumes reasonable values for reflectance and absorption for 1/4-in. pyrex glass, one may show that at 3000°K the temperature drop of the first glass alone is 0.5°K greater than that of the second glass alone when the two are placed in series. This error is small enough to be overlooked in most applications. It would be attractive from the standpoint of reducing reading uncertainties in the glass correction to use more than one additional glass to make the correction. But the errors introduced from multiple reflections increase sharply with the number of glasses used and soon offset the reduced reading uncertainties.

The empirical procedure provides a realistic correction as contrasted to calculations involving known or established transmittances. For example, it was found not to be sufficient, in this case, to calculate the transmittance of the glass at one temperature and then to apply this to establish corrections at other temperatures. It appears that the transmittance changes with brightness, as shown in Table 2. Thus, the empirical procedure conducted over the range of temperatures used in the electron beam furnace was considered the most realistic approach to the correction for glass attenuation.

Coating Attenuation—In contrast to the correction for the attenuation of the glass, the metallic deposits on the glass present a more difficult problem. Heating of the specimen is accomplished by electron beams in a vacuum of 10^{-5} torr, and at very high temperatures metal vapors from the specimen readily deposit themselves on the sight glass. This deposit produces erroneous measurements for which no accurate correction can be made since the thickness of the deposit cannot be predicted. At an initial specimen temperature of 3000°C, a reduction of several hundred degrees is observed in the brightness after only a few minutes. Shutters are usually used and are opened only while taking readings. But this is unsatisfactory for two reasons. Even for short exposures a thin metallic coating will accumulate on the sight glass, possibly too light to notice, and be sufficient to introduce errors. Also, because of the deposit, the temperature cannot be continuously monitored and controlled. By use of suitable shielding arrangements and intermittent reading techniques, these errors are minimized.

Master Calibration Curve—A master calibration curve may be plotted now to give the true temperature from the surface brightness reading of a test specimen. In this procedure, the true temperature of the dummy specimen will be the temperature read in the blackbody holes after adding the sight-port glass correction. At various temperatures and with no coating present, pairs of readings are taken: first, the hole temperature, to which the glass correction is added, and second, the brightness temperature from the surface which simulates the surface of a test specimen. These readings are plotted as a calibration curve in Fig. 4. This curve takes into account all the factors influencing emissivity: material, surface finish, angle of emission, and furnace reflections. The attenuation of the sight glass is also taken into account, so that now if the temperature of a test specimen is desired, one need only read the surface brightness temperature (as measured by the pyrometer) and inspect the curve of Fig. 4 for the corresponding true temperature, provided, of course, that the pyrometer is properly calibrated. A similar curve may be plotted for the determination of the temperature of rod specimens. In this case, the comparison is made

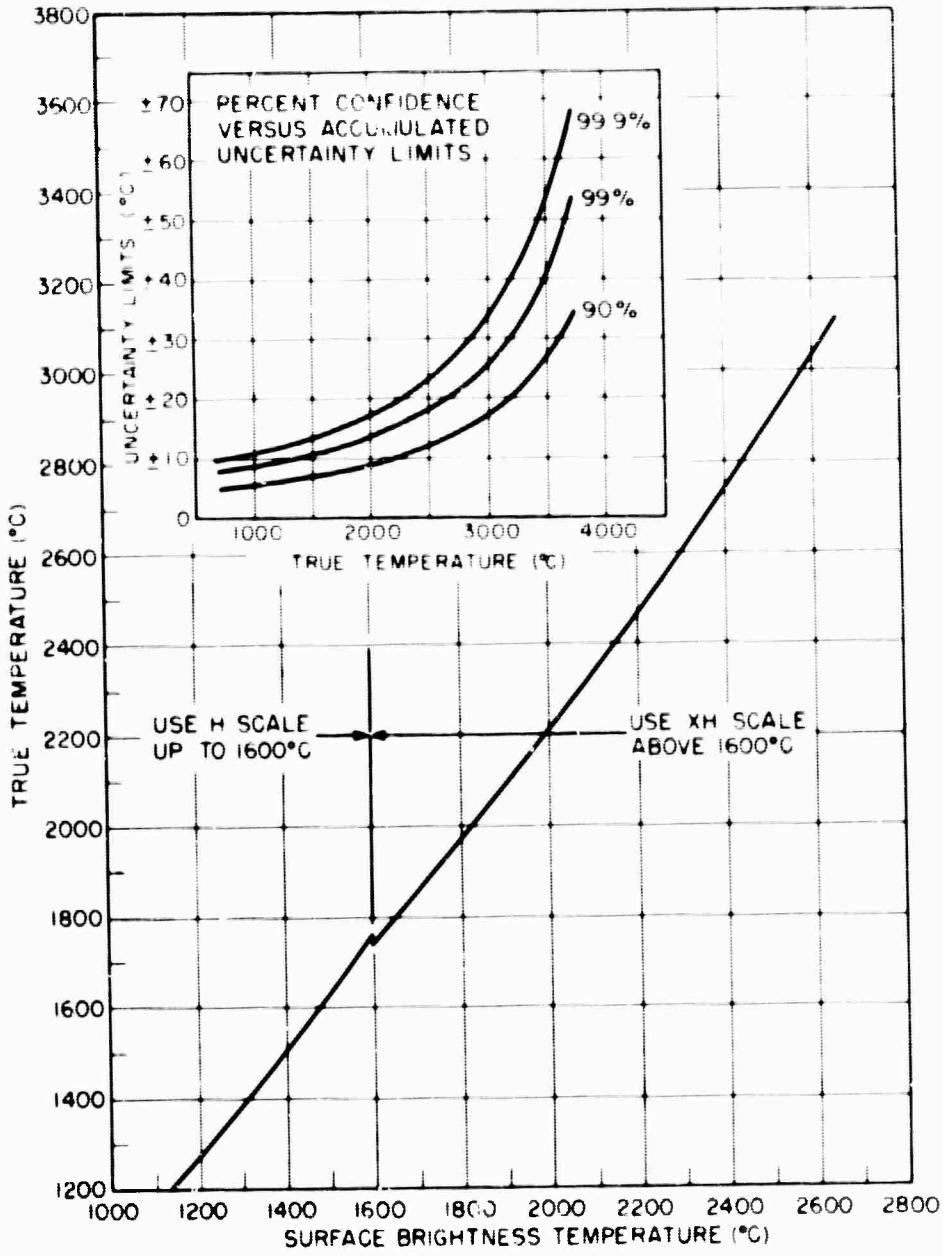

Fig. 4 — Master calibration curve correlating true temperature with surface brightness temperature (Note: This correlation pertains only to readings made with the laboratory pyrometer, Leeds and Northrup, Serial No. 1601797, on a tungsten sheet specimen under the special conditions described in the text. The L & N pyrometer scale has three ranges marked as H (low), XH (medium), and XXH (high).)

between the blackbody hole temperature and the surface brightness temperature directly above or below a hole of the dummy specimen.

Pyrometer Calibration — The laboratory optical pyrometer used in this study to make the measurements for the construction of the curve in Fig. 4 was calibrated against an optical pyrometer that was initially calibrated at the National Bureau of Standards. A list of the indicated temperatures on the pyrometer dial versus the 1948 International Temperature Scale is shown in Table 3. With the use of a tungsten strip-filament lamp, a comparison was made between the readings given by the National Bureau of Standards calibrated pyrometers and the laboratory pyrometer. Although the discrepancies did

TABLE 3
Comparison of NBS and NRL Optical Pyrometer Measurements of Blackbody Temperature

1948 International Temperature Scale (°C)	Scale Reading (°C)					
	Pyrometer Calibrated at NBS (L&N No. 1502596)			NRL Pyrometer (L&N No. 1604797)		
	Low (H) Scale	Medium (XH) Scale	High (XXH) Scale	Low (H) Scale	Medium (XH) Scale	High (XXH) Scale
1200	1196			1193		
1300	1297			1294		
1400	1397			1396		
1500	1496	1497		1497	1510	
1600	1596	1597		1596	1608	
1700	1696	1697		1694	1707	
1800		1797			1812	
1900		1897			1910	
2000		1997			2008	
2200		2197			2210	
2400		2396			2414	
2500		2496	2471		2515	2481
2600		2596	2571		(2616)*	(2582)
2800		2796	2770		(2817)	(2784)
3000			2967			(2985)

*Temperatures in parentheses are extrapolated.

not exceed 0.7 percent in the low (H) range, 0.9 percent in the medium (XH) range, and 1.1 percent in the high (XXH) range, they were numerically high enough so that they could not be overlooked.

The true temperatures shown in Fig. 4 are corrected for the discrepancies noted during pyrometer calibration, so that now readings made with the laboratory optical pyrometer may be applied to Fig. 4 to find the true temperature.

Uncertainties of the Measurements—Even with all the above-mentioned corrections made, Fig. 4 cannot be considered numerically exact because of uncertainties introduced in the reading of the pyrometer. The operator must match the brightness of the internal filament with the brightness of the target as the two images are superimposed. The closeness with which this match can be made depends on the sensitivity of his eye to small changes in the intensity of light, as well as to the color response spectrum of his eye. Exposures to bright light and physiological conditions are known to reduce this sensitivity. The comparison of brightness should be made at a mean effective wavelength of 0.65 micron, but, in fact, the match is made within a bandwidth of about 0.04 micron around this mean wavelength (10). This band arises from the overlap of the eye's color response and the cutoff characteristics of the pyrometer's internal filters. The "color blind" operator may make the intensity match in the wavelength region in which his eye is most sensitive. This may differ from the wavelength around which another operator will make this match. Now, if the spectra of the observed filament and the target are the

same, there is little discrepancy. However, should the spectra differ, which is usually the case, due to the optics and filters in the pyrometer, the intensity matches made by the two operators having different color sensitivity responses will cause differences in readings since the match is not made around the same wavelength.

Brightness match is further made difficult when sighting on targets at nonuniform temperature or on a round target where the brightness increases from its center to either side due to the increase in emissivity as the angle of emission increases. For example, a tungsten rod specimen at 2000°C appears 35°C brighter at the sides than at the center.

By taking a number of readings of an object at constant temperature, the uncertainty limits were established as to how close to a mean temperature the operators at this Laboratory might read the pyrometer. These uncertainty limits are shown in the second column of Table 4 and their meaning should be explained. It will be assumed that actual readings distribute themselves normally about a mean temperature. To define this normal distribution, the mean and the standard deviation are necessary parameters. The mean temperature is the average of a large number of readings. The standard deviation σ, which is a measure of the dispersion (or width) of the function, has the property that 68.3 percent of all the readings made will fall between $+\sigma$ and $-\sigma$. Similarly, 95.5 percent of the readings will fall between $+2\sigma$ and -2σ, and 99.7 percent will fall between $+3\sigma$ and -3σ, etc. Although sufficient data were not available to establish a reliable value of σ for the laboratory pyrometer, the limits shown in the second column of Table 4 are considered to contain 95 percent of the readings so that these limits will be set equivalent to 2σ. Now, if a single reading was taken, *e.g.*, at 3000°K, it would be possible to say how good the odds are that the reading would fall within ±3°, ±6°, and ±9°C away from the mean temperature. Thus, for example, 95.5 percent of the time the reading would lie between the limits of ±6°C of the mean temperature since ±6°C corresponds to $\pm 2\sigma$.

In each step of the procedure used to develop the curve of Fig. 4, readings were taken as follows: First, the laboratory pyrometer was calibrated from the NBS calibrated pyrometer; next, the blackbody holes were read; then the correction for glass was made; the brightness of the dummy specimen's ground flat surface was measured; and finally, the brightness of the test specimen was itself measured. Each reading introduced an uncertainty, and it is the accumulation of these that is plotted as the limits shown in Fig. 4. (The procedure followed in accumulating these uncertainties is discussed in the Appendix.) Thus, for a given surface brightness reading, one can determine between what temperature limits the true temperature will lie 90, 99, or 99.9 percent of the time.

TABLE 4
Measurement Uncertainties for the Calibrated Pyrometer and Reading Uncertainties for The Laboratory Pyrometer

Blackbody Temperature (°K)	Pyrometer Calibrated at NBS* (°K)	NRL Pyrometer† (°K)
1000	±3	±2
2000	±5	±3
3000	±8	±6
4000	±28	±9

*Uncertainty limits in measuring brightness temperature as stated by National Bureau of Standards for the optical pyrometer calibrated by them (Ref. 11)

†Spread of readings (*i.e.*, reading uncertainties) about the mean temperature as calculated from several observations with the laboratory pyrometer

Two-Color Pyrometry

Emissivity—Even though the two-color pyrometer is, in principle, relatively insensitive to both emissivity and the attenuation by glass and coatings, it was found that errors in temperature measurements introduced by these factors were of such magnitude that they could not be neglected. But these errors were, in general, much less than those found in readings made by the optical pyrometer.

In general, emissivity does not affect readings with the two-color pyrometer to the same extent as it does readings with the optical pyrometer. For example, if the true temperature of a polished tungsten target is 2000°C, the optical pyrometer reads 1810°C while the two-color reads 2044°C (9). The error in readings taken with the optical pyrometer is dependent on the logarithm of the spectral emissivity at 0.65 micron (Eq. 3). On the

other hand, for two given spectral emissivities the color temperature T_c and the true temperature T are related, by the following equation derived from Wien's law (12):

$$T_c - T = \frac{2.303\, T_c\, T \log \epsilon_b/\epsilon_r}{C_2(\lambda_r - \lambda_b)/\lambda_r\, \lambda_b} \qquad (4)$$

where $C_2 = 14{,}388$ microns-°K and the subscripts b and r designate the wavelength 0.47 (blue) and 0.64 micron (red), respectively. Thus, the errors to the two-color readings described by Eq. (4), corresponding to those of the optical readings described by Eq. (3), are seen to be proportional to the logarithm of the ratio of the two spectral emissivities. In the case of tungsten at 2000°C, $\epsilon_r = 0.429$* and $\epsilon_b = 0.464$ (7). Now, the smaller error from the two-color pyrometer will be seen from the fact that $|\log (\epsilon_b/\epsilon_r)|$, which equals 0.012, is considerably smaller than $|\log \epsilon_r|$, which equals 0.368. No matter what the magnitude of each spectral emissivity may be, so long as they are close to one another, the reading error from the two-color pyrometer will be small. It may be noticed also that the two-color pyrometer gives a reading higher than true temperature for tungsten because $\epsilon_b > \epsilon_r$ and, thus, the ratio of blue energy to red is greater than that of a blackbody at 2000°C (see Eq. (4)).

The angle of emission ϕ also has an effect on the two-color readings, but again it is less than on optical readings. For example, at 2000°C an increase in the angle of emission ϕ from 30 to 60 degrees causes the apparent brightness to increase by 26°C with the optical pyrometer, while the two-color pyrometer indicates a decrease of 17°C. Figure 3 shows the increase in emissivity for both blue and red radiation, but the ratio of these does not change as greatly as does the emissivity for red alone. Thus the effect on the two-color pyrometer readings should be less than on the optical readings. It is interesting to note from Fig. 3 and Eq. (4) that for an increase of ϕ from 30 to 60 degrees the two-color readings would show a lower temperature since at $\phi = 60$ degrees it sees a decrease in the ratio of blue to red from what it sees at $\phi = 30$ degrees.

Sight Glass and Coating Attenuation—Errors introduced to measurements by the two-color pyrometer are also affected by the selective attenuation of the Pyrex sight glass and the tungsten coatings. These errors are again less than those introduced to optical readings. For example, at 2035°C the glass correction measured by the two-color pyrometer is only 5°C, while that measured by the optical is 20°C. The reduced magnitude of attenuation errors to the two-color measurements is due to the fact that the errors are dependent on the logarithm of the ratio of the transmittances at each wavelength, i.e., on $|\log (\tau_b/\tau_r)|$, and not on $|\log \tau_r|$ alone, as is the case with the optical. In general, as with Pyrex glass, $|\log (\tau_b/\tau_r)|$ is nearer zero than $|\log \tau_r|$.

Tungsten coatings on the sight glass impose a serious problem to continuous temperature measurement with both instruments. However, the errors introduced to readings made by the two-color pyrometer are about one fifth those caused in the optical. But at high temperatures and with the sight glass open for continuous monitoring, the thickness of the coating will increase and cause large errors after long times.

The color temperature T_c and true temperature T are related for given spectral transmittances and emissivities by the following equation extended from Eq. (4):

$$T_c - T = \frac{2.303\, T_c\, T \log (\epsilon_b\, \tau_b/\epsilon_r\, \tau_r)}{C_2(\lambda_r - \lambda_b)/\lambda_r\, \lambda_b} \qquad (5)$$

where $C_2 = 14{,}388$ micron-°K and the subscripts b and r designate the wavelengths 0.47 and 0.64 micron, respectively.

Calibration and Measurement Uncertainties—The two-color pyrometer was calibrated against the NBS standardized pyrometer using a tungsten strip-filament lamp. The uncertainties of readings by the two-color pyrometer are reported (13) for a single reading to be ±1 percent of the span of the scale plus 0.75 percent of the measured temperature. At 2000°K this is calculated as ±19°C, and if it is assumed to be equivalent to three standard deviations, this uncertainty corresponds to accumulated uncertainties of ±13°C for readings taken with the optical pyrometer. It is not entirely clear as to what these reported reading uncertainties refer. The experience at this Laboratory indicates that each time the two-color pyrometer is calibrated against a calibrated optical pyrometer, readings fall within this range of ±19°C. However,

*The small difference in emissivity between that at $\lambda = 0.64$ micron and $\lambda = 0.65$ micron is neglected in this example.

during a given period of operation, the instrument is stable to about ±3° at 2000°K.

Procedure for Temperature Measurement

It was found during the course of this study that each instrument displayed advantages and disadvantages for the various aspects of temperature measurement. Although both the optical and the two-color pyrometer readings were influenced by emissivity and attenuation by the sight glass and coatings, the two-color demonstrated, as expected, far less of an effect. However, over a period of time, the calibration of the two-color varied slightly and the instrument did not demonstrate the same high reproducibility characteristic of the optical. For this reason, the optical pyrometer was selected for the construction of Fig. 4 and for the determination of true temperature.

The two-color pyrometer provides continuous readings and temperature recording. This, together with its reported high sensitivity of less than 1°C and its greater immunity to measurement errors from coatings, made it the desirable choice for temperature monitoring and control.

The procedure finally adopted for temperature measurement is as follows. Before a test is begun, the test specimen is heated to the desired temperature as measured with the optical pyrometer through clean sight glass in accordance with the correlation of Fig. 4. At this point in the procedure, it is important to minimize the coating errors, and to this end the following arrangement was found convenient and useful. A circular disc, with a pie-shaped sector removed, is so constructed that it can be rotated by a magnetic couple from outside the sight glass. After a test specimen has been heated to the desired temperature, the disc can be rotated so as to expose a clean section of glass and permit a final reliable reading before the test is begun.

When this final reading with the optical pyrometer is taken, the corresponding reading on the two-color pyrometer is noted, and control of the electron beams is adjusted to keep this temperature constant throughout the test. However, a serious limitation to this procedure arises from the selective attenuation of the tungsten coating on the sight glass. At high temperatures and for long times, even the two-color pyrometer readings drop to where one may only estimate the temperature of the specimen. Despite this limitation, the overall procedure was found satisfactory in most tests and took advantage of the best characteristics of both instruments.

SUMMARY

The application of both the optical and the two-color pyrometers was investigated for the measurement of temperature of a test specimen in the electron beam furnace. By using the optical pyrometer an empirical correlation was established between a blackbody temperature and the corresponding brightness of a surface similar to that of a test specimen. This correlation, which was plotted as a calibration curve, accounted for all the error-producing factors of emissivity and attenuation of sight glass, as well as those due to instrument calibration and uncertainties. The temperature of a test specimen could then be determined from its surface brightness temperature using this correlation. However, the presence of coatings of metallic vapor on the sight glass of the furnace introduced an error that could not be exactly accounted for, but rather only minimized.

Both the optical and the two-color pyrometers were compared with regard to the influence of emissivity and attenuation on their readings, as well as to their accuracy and reproducibility. The two-color pyrometer readings were affected by emissivity and attenuation by glasses and coatings, but to a lesser degree than were those of the optical pyrometer. However, the stability and accuracy of the optical pyrometer were found superior. Thus, it was not desirable to use either instrument by itself to determine and control temperature in the electron beam furnace. Rather, the following procedure was established to take advantage of the best characteristics of both instruments. Because of its high accuracy and stability, the optical pyrometer was selected to establish the true temperature of a specimen. The two-color pyrometer, although not as stable or accurate, provided continuous readings and recording with high sensitivity. It was also less sensitive to the presence of metallic coatings on the sight glass. For these reasons the two-color pyrometer was selected for temperature monitoring and control.

ACKNOWLEDGMENTS

The authors wish to express their thanks to Mr. H. J. Bixhorn for assistance with the statistical portion of the study and to Mr. J. T. Atwell for assistance with various phases of the work. Also the authors are indebted to Dr. M. R. Achter for reviewing the manuscript.

REFERENCES

1. Kostkowski, H.J., and Lee, R.D., "Theory and Methods of Optical Pyrometry," Natl. Bur. Standards, Monograph 41, Mar. 1, 1962
2. Hill, W.E., "Two-Color Pyrometry," in "Temperature, Its Measurement and Control in Science and Industry," Vol. 3 (Part 2), p. 419, New York:Reinhold, 1962
3. Ackerman, S., "Notes on the Design and Performance of a Two-Color Pyrometer," in "Temperature, Its Measurement and Control in Science and Industry," Vol. 3 (Part 2), p. 849, New York:Reinhold, 1962
4. DeVos, J.C., "Evaluation of the Quality of a Blackbody," *Physica*, **20**:669 (1954)
5. Casselton, R.E.W., Erez, G., and Quinn, T.J., "Black-Body Radiation from Partially Enclosed Cavities," *J. Inst. Metals* **91**:408 (1963)
6. Smithells, C.J., ed., "Metals Reference Book," Vol. 2, p. 659, New York:Interscience, 1955
7. Smithells, C.J., "Tungsten, Its Metallurgy, Properties and Applications," New York:Chemical Publishing Co., 1953
8. Allen, R.D., Glaser, L.E., Jr., and Jordan, P.L., "Spectral Emissivity, Total Emissivity, and Thermal Conductivity of Molybdenum, Tantalum, and Tungsten above 2300°K," *J. Appl. Phys* **31**:1382 (1960)
9. "Handbook of Chemistry and Physics," p. 2720, (38th ed.), Cleveland:Chemical Rubber Co., 1956
10. Gray, W.T., "Precision and Accuracy in Radiation Pyrometry," Leeds and Northrup Company, Philadelphia, Pa., 1963
11. Private communication accompanying the N.B.S. calibrated pyrometer, Serial No. 1502596
12. Instrument Development Laboratories, Inc., Instruction Manual No. 5037-B for Pyro-Eye, Attleboro, Mass.
13. Instrument Development Laboratories, Inc., Bulletin 613, Attleboro, Mass.

Appendix

Accumulation of Uncertainties

In establishing the correlation between surface brightness and true temperature, as previously shown in Fig. 4, a series of pyrometer readings, each containing an uncertainty, was made. In order to accumulate the total uncertainty, it is necessary to identify the distribution and magnitude of the individual uncertainties inherent in each measurement. Estimates and assumptions concerning these distributions were made since sufficient data were not available to establish them accurately. Once these distributions are set, the accumulation is done by standard statistical techniques.

Temperature measurement uncertainties are introduced by (a) the measurement uncertainties of the pyrometer calibrated at the National Bureau of Standards (NBS) and (b) the reading uncertainties introduced when calibrating the laboratory pyrometer (Table 4) against the NBS pyrometer. Further uncertainties are introduced in reading the blackbody temperature, in readings made for the attenuation corrections for the furnace sight-port glass, and in reading the surface brightness of the dummy specimen and of the test specimen. So the accumulated uncertainties pertaining to the calibration curve of Fig. 4 should be examined.

It will be assumed that the reading uncertainties and the uncertainties stated by NBS are distributed normally about a mean temperature measurement. The mean temperature measurement of the NBS-calibrated pyrometer is assumed to be the true temperature (when measuring a blackbody) to this extent: the average of a large number of calibrations and measurements would tend to approach the true temperature. Next, it is considered reasonable to suppose that 99.5 percent of the measurements made with the pyrometer calibrated at NBS should fall within the limits stated by them. Therefore, these limits (first column of Table 4) will be considered equivalent to three standard deviations (3σ). Similarly, the reading uncertainties of the laboratory pyrometer, as stated in the second column of Table 4, are considered to contain only 95 percent of readings made; so these limits will be set equivalent to 2σ.

Now one can evaluate the limits $\pm\sigma$, $\pm 2\sigma$, $\pm 3\sigma$, etc., for the accumulated uncertainties at

each temperature of Table 4 and assign the probability of falling within these limits when using the calibration curve in Fig. 4. For simplicity let

a = uncertainty limits of brightness measurements using the NBS-calibrated pyrometer (equivalent to three standard deviations), and

b = uncertainty limits of readings by the laboratory pyrometer (equivalent to two standard deviations).

The variance σ^2 is defined as the square of the standard deviation σ. When calibrating an instrument against a standardized one, it may be shown that the variance of readings taken with the instrument equals the sum of the variance of the standard and the variance of the instrument. Thus the variance for the calibrated laboratory pyrometer is $[(a/3)^2 + (b/2)^2]$. The construction of Fig. 4 is expressed algebraically as

$$T_{true} = T\begin{pmatrix}\text{test}\\ \text{specimen}\\ \text{surface}\end{pmatrix} + \Bigg[\, T\begin{pmatrix}\text{black-}\\ \text{body}\end{pmatrix} + T\begin{pmatrix}\text{glass}\\ \text{correction}\end{pmatrix} - T\begin{pmatrix}\text{dummy}\\ \text{specimen surface}\end{pmatrix}\Bigg]. \tag{A1}$$

Since this relationship represents the addition or subtraction of independent temperature readings, the variances of each reading may be added to give the total variance of the true temperature. By taking the average of n independent readings instead of a single reading, each variance of a contributing reading is divided by n. The following listing gives the variance associated with each reading made for the construction of Fig. 4.

Temperature Reading	Variance (σ^2) of the Reading
Test Specimen Surface	$\left(\frac{a^2}{9} + \frac{b^2}{4}\right)$
Blackbody (average of n_1 readings)	$\frac{1}{n_1}\left(\frac{a^2}{9} + \frac{b^2}{4}\right)$
Glass Correction (average of n_2 readings)	$\frac{2}{n_2}\left(\frac{a^2}{9} + \frac{b^2}{4}\right)$
Dummy Specimen surface (average of n_3 readings)	$\frac{1}{n_3}\left(\frac{a^2}{9} + \frac{b^2}{4}\right)$
Total Variance of True Temperature Measurement	$\left(1 + \frac{1}{n_1} + \frac{2}{n_2} + \frac{1}{n_3}\right)\left(\frac{a^2}{9} + \frac{b^2}{4}\right)$

Thus the standard deviation σ for the true temperature of Fig. 4 is

$$\left(1 + \frac{1}{n_1} + \frac{2}{n_2} + \frac{1}{n_3}\right)^{1/2}\left(\frac{a^2}{9} + \frac{b^2}{4}\right)^{1/2} \tag{A2}$$

Evaluating Eq. (A2) with the a and b for each temperature shown in Table 4, values are obtained for $\pm\sigma$, $\pm 2\sigma$, etc., as shown in Table A1 when $n_1 = n_3 = 1$ and $n_2 = 2$. The uncertainty limits shown in Table 4 are extended from the values shown in Table A1. Suitable multiples of σ are selected to give the limits (Table A2) between which 90, 99, and 99.9 percent of true temperature determinations should fall.

TABLE A1
Accumulated Uncertainties for Master Calibration Curve (Fig. 4)

Blackbody Temperature (°K)	$\pm\sigma$ $P = 68.3\%$* (°K)	$\pm 2\sigma$ $P = 95.5\%$ (°K)	$\pm 3\sigma$ $P = 99.7\%$ (°K)
1000	2.8	5.7	8.5
2000	4.4	8.9	13.3
3000	8.0	16.1	24.1
4000	20.7	41.4	62.2

*P is the probability that a reading will fall within the limits $\pm\sigma$, $\pm 2\sigma$, or $\pm 3\sigma$.

Note: These uncertainties apply only to the curve of Fig. 4 for brightness readings taken with the Laboratory Pyrometer.

TABLE A2
Summary of Unknown Systematic Errors
and Accumulated Uncertainties

Type of Error	Amount of Error			
	at 1000°K (°K)	at 2000°K (°K)	at 3000°K (°K)	at 4000°K (°K)
Unknown Systematic Errors:				
1. Blackbody assumption				
a. best (DeVos (4))	− 1*	− 2	− 4	− 7
b. worst (Casselton *et al.* (5))	− 6	− 26	− 57	− 103
2. Vapor deposit on glass (X = temperature drop for any given deposit at 1000°K)	$-X$	$-4X$	$-9X$	$-16X$
Accumulated Uncertainties: for:				
$P = 90\%$† (1.645σ)	± 5	± 7	± 13	± 34
$P = 99\%$ (2.575σ)	± 7	± 11	± 21	± 53
$P = 99.9\%$ (3.29σ)	± 9	± 15	± 26	± 68

*+ means higher than true temperature.
− means lower than true temperature.
†P is the probability that a reading will fall within the limits indicated.